Neural-Network-Based Variable Structure Control of Electrohydraulic Servosystems Subject to Huge Uncertainties Without Persistent Excitation

Chih-Lyang Hwang, *Associate Member, IEEE*

***Abstract*—A novel scheme investigating a radial-basis-function neural network (RBFNN) with variable structure control (VSC) for electrohydraulic servosystems subject to huge uncertainties is presented. Although the VSC possesses some advantages (e.g., fast response, less sensitive to uncertainties, and easy implementation), the chattering control input often occurs. The reason for a chattering control input is that the switching control in the VSC is used to cope with the uncertainties. The larger the uncertainties which arise, the larger switching control occurs. In this paper, an RBFNN is employed to model the uncertainties caused by parameter variations, friction, external load, and controller. A new weight updating law using a revision of e-modification by a time-varying dead zone can achieve an exponential stability without the assumption of persistent excitation for the uncertainties or radial basis function. Then, an RBFNN-based VSC is constructed such that some part of uncertainties are tackled, that the tracking performance is improved, and that the level of chattering control input is attenuated. Finally, the stability of the overall system is verified by the Lyapunov stability criterion.**

***Index Terms*— Electrohydraulic servosystems, persistent excitation, radial-basis-function neural network, variable structure control.**

I. Introduction

THE development of reliable electrohydraulic elements interfaced to microcontrollers has been the most significant factor in the renaissance of the hydraulic systems. The electrohydraulic servovalves serve as interfaces between the electrical devices and the hydraulic system. They are capable of converting the low-power electrical inputs into the movement of spools to precisely control a large-power low-speed hydraulic actuator. For instance, they are used extensively in such applications as computer numerical control machine tools, aircraft, ship steering gear, and test machinery [1]–[5]. However, some nonlinear time-varying phenomena, such as the relationship between input current and output flow, fluid compressibility, deadband due to the internal leakage and hysteresis, friction in the cylinder (or hydraulic motor), and external load [6], [7], make the control or modeling of hydraulic systems difficult.

Manuscript received July 14, 1997; revised February 11, 1998 and June 12, 1998. Recommended by Technical Editor K. Ohnishi. This work was supported in part by the National Science Council of Taiwan, R.O.C., under Grant NSC-87-2218-E-036-001.

The author is with the Department of Mechanical Engineering, Tatung Institute of Technology, Taipei, 10451 Taiwan, R.O.C.

Publisher Item Identifier S 1083-4435(99)02311-X.

The controller designs for these control systems can be variable structure control (VSC) (e.g., [8] and [9]), adaptive control (e.g., [10] and [11]), and fuzzy control. The distinct controller has its own advantages and disadvantages. Although VSC provides a robust means for controlling a nonlinear dynamic system with uncertainties, it always results in a chattering control input due to its discontinuous switching control used to deal with the uncertainties. The larger the uncertainties which take place, the larger is the switching control which occurs. The chattering control input has some drawbacks, e.g., easy damage of mechanism and excitation of unmodeled dynamics. Hence, how to obtain a chattering-free VSC with an acceptable tracking result for the electrohydraulic servosystems subject to enormous uncertainties becomes an important topic.

The most commonly used method for attenuating the chattering control input is the boundary layer method [12]–[15]. Indeed, the control input is smoother than that without using a boundary layer. However, its stability is guaranteed only outside of the boundary layer, and its tracking error is bounded by the width of boundary layer [12]–[15]. In this paper, a radial-basis-function neural network (RBFNN) is employed to model the uncertainties caused by parameter variations, friction, external load, and controller. Then, an RBFNN-based VSC with time-varying switching gain and boundary layer [9] is designed such that some part of the uncertainties are tackled, that the tracking performance is improved, and that the level of chattering control input is attenuated. The reason to use an RBFNN but not to use another neural network (e.g., multilayer neural network [16]) is that the RBFNN results in the nonlinear maps in which the connection weights occur linearly. Hence, the stability of the overall system is not difficult to accomplish, the updating law for adjusting is substantially simplified, and the convergence of connection weights is rapid [7], [17]–[19]. Furthermore, many papers examine the neuro control or neural network modeling for nonlinear systems [20]–[23].

Numerous papers discussing adaptive control for the system in the presence of disturbances were given one or two decades ago. For example, a dead zone in the adaptive law [24]–[26] guarantees the boundedness of all the signals in the adaptive loop. In addition, [24], as well as [26], restrict the search region of parameter space by using *a priori* information about the bound of parameter. An extra term of the form $-\sigma\theta$ in the adaptive law for adjusting the parameter θ introduced in [27] is referred to as σ-modification. In [28], an e-modification

is designed to improve the performance of the system in all respects, while retaining the advantage of assuring robustness in the presence of disturbances without the requirement of persistent excitation (PE). In this paper, a revision of e-modification using a time-varying dead zone is employed to achieve an exponential stability without the assumption of PE for the uncertainties. Whatever the uncertainties which occur, its assumption about PE is not assigned so that the controller design is more practical because of the difficulty of satisfying the PE condition in an RBFNN [29]. Hence, without the assumption of PE [16], [29], the proposed updating law can force the connection weights of the RBFNN into the vicinity of their optimal values. Together with the robustness of VSC, the control performance of an electrohydraulic servosystem in the presence of huge uncertainties is excellent.

II. Problem Formulation

First, the dynamics of an electrohydraulic servosystem is considered as follows. The relationship between the servovalve displacement $x_v(t)$ (m) and the load flow $Q_l(t)$ (m^3/s) is described in the following servovalve equation:

$$Q_1(t) = K_g(t)x_v(t) - K_c P_l(t) \tag{1}$$

where K_c denotes the servovalve flow-pressure coefficient (m^3/s/MPa), $P_l(t)$ stands for the load differential pressure (MPa), and $K_g(t)$ is called the servovalve flow gain, given by

$$K_g(t) = C_d A_g \sqrt{[P_s - \mathrm{sgn}(x_v)P_l(t)]/\rho} \tag{2}$$

where C_d denotes the discharge coefficient (dimensionless), A_g is the area of gradient (m), ρ represents the fluid mass density (kg/m^3) and P_s is the supply pressure (Mpa). The continuity equation to the hydraulic motor chamber gives

$$Q_l(t) = D_m\dot{\theta}_m(t) + C_{tm}P_l(t) + (V_t/4\beta_e)\dot{P}_l(t) \tag{3}$$

where D_m is the volumetric displacement of the motor (m^3/rad), $\theta_m(t)$ is the angular position of the motor shaft (rad), C_{tm} denotes the total leakage coefficient of the motor (m^3/s/MPa), V_t is the total compressed volume (m^3), and β_e denotes the effective bulk modulus of the system (MPa). The torque balance equation for the motor is depicted as follows:

$$P_l(t)D_m = J_t\ddot{\theta}_m(t) + B_m\dot{\theta}_m(t) + G\theta_m(t) + T_l(t,\theta_m,\dot{\theta}) \tag{4}$$

where J_t denotes the total inertia of the motor and load (m·N·s^2), B_m is the viscous damping coefficient of the load (m·N·s), G denotes the torsional spring gradient of the load, and the uncertain load is symbolized by $T_l(t,\theta_m,\dot{\theta}_m)$ (m·N) which can be external load, stick–slip friction, Coulomb friction, and Stribeck friction [6], [7]. Substituting (1) into (3) gives

$$K_g(t)x_v(t) = D_m\dot{\theta}_m(T) + K_{\mathrm{ce}}P_l(t) + (V_t/4\beta_e)\dot{P}_l(t) \tag{5}$$

where $K_{\mathrm{ce}} = K_c + C_{tm}$ denotes the total flow-pressure coefficient (m^3/s/MPa). Furthermore, the relationship between the servovalve displacement and the applied voltage to servovalve is described as follows:

$$x_v(t) = K_v u(t) \tag{6}$$

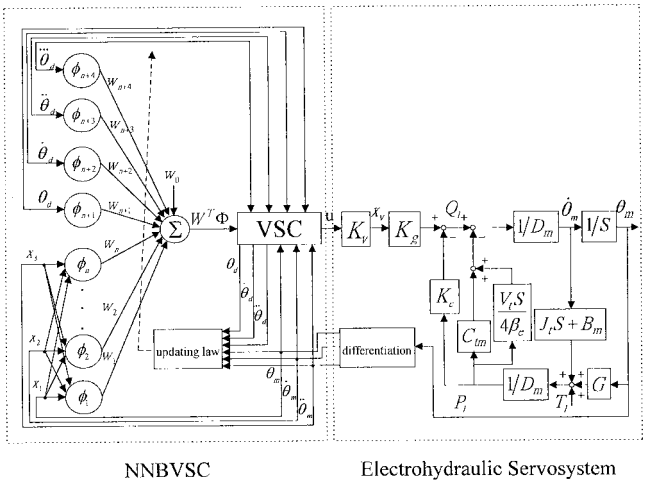

Fig. 1. The control block diagram of the overall system.

where K_v is the servovalve gain. Define the following state variables:

$$x(t) = [x_1(t) \quad x_2(t) \quad x_3(t)]^T = [\theta_m(t) \quad \dot{\theta}_m(t) \quad \ddot{\theta}_m(t)]^T. \tag{7}$$

Then, the state variable equation describing the dynamics of the electrohydraulic servosystems is achieved as follows:

$$\begin{aligned}\dot{x}_1(t) &= x_2(t)\\ \dot{x}_2(t) &= x_3(t)\\ \dot{x}_3(t) &= -a_1(t)x_1(t) - a_2(t)x_2(t) - a_3(t)x_3(t)\\ &\quad + b(t)u(t) - d(t)\end{aligned} \tag{8}$$

where

$$\begin{aligned}a_1(t) &= 4\beta_e K_{\mathrm{ce}}G/(V_t J_t)\\ a_2(t) &= G/J_t + 4\beta_e D_m^2/(V_t J_t)\\ &\quad + 4\beta_e K_{\mathrm{ce}}B_m/(V_t J_t)\\ a_3(t) &= B_m/J_t + 4\beta_e K_{\mathrm{ce}}/V_t\\ b(t) &= 4\beta_e D_m K_g(t)K_v/(V_t J_t) > 0 \quad \forall t\\ d(t) &= 4\beta_e K_{\mathrm{ce}}T_l(t,\theta_m,\dot{\theta}_m)/(V_t J_t)\\ &\quad + \dot{T}_l(t,\theta_m,\dot{\theta}_m)/J_t.\end{aligned} \tag{9}$$

The objective of this paper is to design a radial-basis-function neural-network-based VSC (NNBVSC) for the electrohydraulic servosystems (see Fig. 1) subject to huge uncertainties resulting from $a_i(t)$ $(1 \le i \le 3)$, $b(t)$, $d(t)$, and the controller itself which are not necessarily PE. Without the occurrence of a chattering control input, the angular position $\theta_m(t)$ tracks the desired angular position $\theta_d(t)$ as close as possible.

III. Controller Development

The design procedure of the VSC is a two-stage process [7]–[9], [12]–[14]. The first phase is to choose a switching surface which is stable and has a desired behavior. The second phase is to determine a control law that forces the system's trajectory into the neighborhood of switching surface

satisfying some conditions such that an asymptotical tracking can be guaranteed [9]. In the following section, the traditional VSC for the electrohydraulic servosystem is first discussed.

A. Traditional VSC

Define the following switching surface:

$$\sigma(t) = \ddot{e}(t) + p_1\dot{e}(t) + p_2 e(t) + p_3 \int_0^t e(\tau)\,d\tau,$$
$$e(t) = \theta_d(t) - x_1(t) \tag{10}$$

where p_i $(1 \le i \le 3)$ are chosen such that the dynamics of $\sigma(t) = 0$ are stable and have the desired eigenvalues. The assumptions of this section are described as follows.

A1) $a_i(t) = \bar{a}_i(t) + \Delta a_i(t),\ |\Delta a_i(t)| \le \alpha_i(t) \quad \forall t,$
$b(t) = \bar{b}(t) + \Delta b(t), \quad |\Delta b(t)| \le \beta(t) < \bar{b}(t) \quad \forall t.$

A2) $|d(t)| < \gamma(t) \quad \forall t.$

A3) $\{\dddot{\theta}_d(t), \ddot{\theta}_d(t), \dot{\theta}_d(t), \theta_d(t)\}$ are known, bounded, and continuous.

A4) $x(t)$ is available.

Remark 1: Assumption A1 reveals that the nominal system parameters and the upper bound of parameter uncertainties are known. Similarly, Assumption A2 indicates that an upper bound of uncertain dynamic load is known. However, if the system uncertainties are huge, the information of $\alpha_i(t)$ $(1 \le i \le 3)$ or $\beta(t)$ or $\gamma(t)$ is difficult to obtain because overconservative design of the controller makes the system response oscillatory or even unstable [12]–[15]. If all the states are not available, an observer combined with a controller can be employed to deal with this kind of control problem (see, e.g., [19]).

The following theorem discusses the traditional VSC for the electrohydraulic servosystem (8), (9) under Assumptions A1–A4.

Theorem 1: Consider the electrohydraulic servosystem (8), (9) and the following VSC (11):

$$u(t) = u_{\rm eq}(t) + u_{\rm sw}(t) \tag{11}$$

with

$$u_{\rm eq}(t) = \{\dddot{\theta}_d(t) + \bar{a}_1(t)x_1(t) + \bar{a}_2(t)x_2(t) + \bar{a}_3(t)x_3(t) + p_1[\ddot{\theta}_d(t) - x_3(t)] + p_2[\dot{\theta}_d(t) - x_2(t)] + p_3[\theta_d(t) - x_1(t)]\}/\bar{b}(t) \tag{12}$$

$$u_{\rm sw}(t) = k(x,t)\,\mathrm{sgn}(\sigma) \tag{13}$$

where

$$k(x,t) = [\alpha_1(t)|x_1(t)| + \alpha_2(t)|x_2(t)| + \alpha_3(t)|x_3(t)| + \gamma(t) + \beta(t)|u_{\rm eq}(t)|]/[\bar{b}(t) - \beta(t)]. \tag{14}$$

Under Assumptions A1–A4, $x_1(t)$ asymptotically follows $\theta_d(t)$ and $\{u(t)\}$ is bounded.

Proof: See [9] for a similar result. □

Remark 2: The symbol $\mathrm{sgn}(\sigma)$ in (13) can be modified as $\mathrm{sat}(\sigma/\mu)$, where μ denotes a constant width of boundary layer, to reduce the chattering control input. However, its stability is guaranteed only outside of the boundary layer, and its tracking error is bounded by the width of boundary layer [12]–[15].

B. RBFNN-Based VSC

From the result of *Theorem 1*, if the upper bound of system uncertainties (i.e., $\sum_{i=1}^{3}\alpha_i(t)|x_i(t)|$ or $\beta(t)|u_{\rm eq}(t)|$) or uncertain dynamic load (i.e., $\gamma(t)$) is tremendous, the switching gain $k(x,t)$ is large. Then, the chattering control input results from (13). Under this circumstance, the magnitude or change rate of control input may exceed the limited value of the servovalve, the system stability is possibly not guaranteed and the system performance is poor. Although the boundary layer method can attenuate the degree of chattering control input, its stability is ensured only outside of the boundary layer. Hence, the asymptotical tracking often cannot be attained. The main reason of resulting in a large switching gain is due to the poor modeling. Besides the original modeling of the electrohydraulic servosystem, the modeling of system uncertainties or uncertain dynamic load or uncertainties caused by the controller should be established for the controller design. Then, the switching gain in (14) is reduced; the level of chattering control input is attenuated. This is the motivation of this paper. Before designing the proposed controller, the condition for the operating point to converge into the origin is described in the sequence.

First, the dynamics of the switching surface (10) can be rewritten as follows:

$$\dot{E}(t) = PE(t) + Q\sigma(t) \tag{15}$$

where

$$E(t) = \begin{bmatrix} \int_{t_0}^{t} e(\tau)\,d\tau \\ e(t) \\ \dot{e}(t) \end{bmatrix}, \quad P = \begin{bmatrix} 0 & 1 & 0 \\ 0 & 0 & 1 \\ -p_3 & -p_2 & -p_1 \end{bmatrix}$$
$$Q = \begin{bmatrix} 0 \\ 0 \\ 1 \end{bmatrix}. \tag{16}$$

Then, the solution of (15) is described as follows:

$$E(t) = \exp[P(t-t_0)]E(t_0) + \int_{t_0}^{t} \exp[P(t-\tau)]Q\sigma(\tau)\,d\tau, \quad t \ge t_0. \tag{17}$$

Because the dynamics of the switching surface (15) are stable, there exist two positive constants K_1 and K_2 such that

$$\|\exp[P(t-t_0)]\| \le K_1 \exp[-K_2(t-t_0)] \quad \forall t \ge t_0 \ge 0, \quad K_2 = -\max_{1\le i\le 3} \Re e\{\lambda_i[P]\}. \tag{18}$$

The following theorem examines the stability of switching surface as $|\sigma(t)| \ne 0$.

Theorem 2: If the dynamics of the switching surface (15) satisfy the following inequality $|\sigma(t)| < \alpha\|E(t)\|$ for $t \ge t_0$, where $0 < \alpha < K_2/K_1$, and its initial condition $E(t_0)$ is bounded, then $e(t) \to 0$ with a rate $(K_2 - \alpha K_1)$ as $t \ge t_0$.

Proof: See [7] or [9] for a similar result. □

Remark 3: Based on the Cayley–Hamilton Theorem, the matrix $e^{P(t-t_0)}$ can be expressed as a 3×3 matrix. Then, from (18), K_1 and K_2 can be determined; hence, the value of α is found because $0 < \alpha < K_2/K_1$. If the poles of the P

matrix are all assigned at the more left region of the S plane, the value of α becomes smaller.

The following assumption is required for the derivation of the proposed controller in *Theorem 3*.

A5) The system uncertainties caused by parameter variations, external load, tracking error, and controller are continuous, bounded, but unknown. They can be approximated by the following neural network:

$$\sum_{i=1}^{3}\Delta a_i(t)x_i(t)-\Delta b(t)u_{\rm eq}(t)+d(t)-\xi(t)=\bar{W}^T\Phi(x,z)+\varepsilon(t,x,z),\quad \forall t \tag{19}$$

where $\xi(t)=[\bar{\alpha}E^T(t)\dot{E}(t)\,\mathrm{sgn}(\sigma)]/\|E(t)\|$ (where $0<\bar{\alpha}<\alpha$), $x(t)$ and $z(t)=[\theta_d(t)\ \ \dot{\theta}_d(t)\ \ \ddot{\theta}_d(t)\ \ \dddot{\theta}_d(t)]^T\in\Omega(x,z)$ which is a compact set $\in\Re^3\times\Re^4$, $\Phi(x,z)$ denotes a modified radial basis function

$$\begin{aligned}&\Phi(x,z)\\&\quad=[1\quad\phi_1(x)\ \cdots\ \phi_n(x)\quad\phi_{n+1}(z)\ \cdots\ \phi_{n+4}(z)]^T\\&\phi_i(x)\\&\quad=\exp\left[-\|x(t)-c_i\|^2/\delta_i^2\right],\quad i=1,\cdots,n\\&\phi_{n+1}(z)\\&\quad=\theta_d(t),\quad \phi_{n+2}(z)=\dot{\theta}_d(t)\\&\phi_{n+3}(z)\\&\quad=\ddot{\theta}_d(t),\quad \phi_{n+4}(z)=\dddot{\theta}_d(t).\end{aligned} \tag{20}$$

$\bar{W}\in\Re^{n+5}$ represents an unknown but fixed vector satisfying the following inequality:

$$\|\bar{W}\|\le W_{\max} \tag{21}$$

and $\varepsilon(t,x,z)$ is unknown, but bounded. Furthermore, it is relatively bounded by the following inequality [26]:

$$|\varepsilon(t,x,z)|\le\varepsilon_0\|\Phi(x,z)\|+\varepsilon_1,\quad x,z\in\Omega(x,z),\quad\forall t. \tag{22}$$

Remark 4: The selection of radial basis function in (20) is due to the fact from (19), (24), (9) and

$$\begin{aligned}|\xi(t)|&\le\bar{\alpha}[e^2(t)+\dot{e}^2(t)+\ddot{e}^2(t)]^{1/2}\\&\le\bar{\alpha}[|e(t)|+|\dot{e}(t)|+|\ddot{e}(t)|].\end{aligned}$$

Hence, the number of radial basis function is reduced.

The following theorem is the main result of this paper.

Theorem 3: Consider the system (8) and (9) and the control law (23)

$$u(t)=u_{\rm eq}(t)+u_{\rm sw}(t) \tag{23}$$

with

$$\begin{aligned}u_{\rm eq}(t)=\{&\dddot{\theta}_d(t)+\bar{a}_1(t)x_1(t)+\bar{a}_2(t)x_2(t)\\&+\bar{a}_3(t)x_3(t)+p_1[\ddot{\theta}_d(t)-x_3(t)]\\&+p_2[\dot{\theta}_d(t)-x_2(t)]\\&+p_3[\theta_d(t)-x_1(t)]+W^T(t)\Phi(x,z)\}/\bar{b}(t)\end{aligned} \tag{24}$$

$$\begin{aligned}u_{\rm sw}(t)=\{&\gamma_1\sigma_\Delta(t)+\gamma_2(t)\sigma_\Delta(t)/[|\sigma_\Delta(t)|\\&+\mu(t)]\}/[\bar{b}(t)-\beta(t)]\end{aligned} \tag{25}$$

where

$$\dot{W}(t)=\sigma_\Delta(t)H^{-1}\Phi(x,z)-\eta|\sigma_\Delta(t)|H^{-1}W(t) \tag{26}$$

$\sigma_\Delta(t)$ is defined in (27), shown at the bottom of the page,

$$H=\mathrm{diag}\{h_{ii}\},\quad h_{ii},\eta>0,\quad 0\le i\le n+4 \tag{28}$$

$$f_1(t)=\left\{\mu(t)+\frac{\gamma_2(t)}{\gamma_1}-\frac{\eta W_{\max}^2}{4\gamma_1}-\frac{\varepsilon_0\|\Phi(x,z)\|+\varepsilon_1}{\gamma_1}\right\}\Big/2 \tag{29}$$

$$f_2(t)=\frac{\eta W_{\max}^2\mu(t)}{4\gamma_1}+\frac{[\varepsilon_0\|\Phi(x,z)\|+\varepsilon_1]\mu(t)}{\gamma_1}>0 \tag{30}$$

$$f(t)=\sqrt{f_1^2(t)+f_2(t)}-f_1(t)\ge 0 \tag{31}$$

and (32), shown at the bottom of the page. The overall system satisfies the following conditions: 1) a stable switching surface (10); 2) $\|\bar{W}-W(0)\|<\rho_1,\|x(0)\|<\rho_2$; 3) Assumptions A1–A5; and 4) $f(t)+\bar{\alpha}\|E(t)\|<\alpha\|E(t)\|<\{\eta W_{\max}^2/4+\varepsilon_0\|\Phi(x,z)\|+\varepsilon_1\}/\gamma_1+\bar{\alpha}\|E(t)\|$. The controller (23) is employed to the system (8) and (9), then $|\sigma_\Delta(t)|<f(t)$, $\{W(t),u(t)\}$ are bounded and $e(t)\to 0$ with a rate $(K_2-\alpha K_1)$ as $t\to\infty$.

Proof: See the Appendix. □

Remark 5: According to the result (32), one reasonable choice of time-varying boundary layer $\mu(t)$ is expressed as follows:

$$\begin{aligned}0<\mu(t)&=(\alpha-\bar{\alpha})\|E(t)\|\\&\cdot\left\{\frac{\gamma_2(t)-\left[\eta W_{\max}^2/4+(\varepsilon_0\|\Phi(x,z)\|+\varepsilon_1)\right]}{\left[\eta W_{\max}^2/4+(\varepsilon_0\|\Phi(x,z)\|+\varepsilon_1)\right]}\right\}.\end{aligned} \tag{33}$$

$$\sigma_\Delta(t)=\begin{cases}\sigma(t)-\Delta(t)\,\mathrm{sgn}(\sigma), & \text{if } |\sigma(t)|>\Delta(t)=\bar{\alpha}\|E(t)\|>0,\ \text{where } \bar{\alpha}<\alpha\\ 0, & \text{otherwise}\end{cases} \tag{27}$$

$$0<\mu(t)<(\alpha-\bar{\alpha})\|E(t)\|\cdot\left\{\frac{\gamma_2(t)/\gamma_1}{\eta W_{\max}^2/4\gamma_1+[\varepsilon_0\|\Phi(x,z)\|+\varepsilon_1]/\gamma_1-(\alpha-\bar{\alpha})\|E(t)\|}-1\right\} \tag{32}$$

To ensure $\mu(t) > 0$, the following selection of time-varying switching gain $\gamma_2(t)$ is given

$$\gamma_2(t) = \eta W_{\max}^2/4 + \varepsilon_0\|\Phi(x,z)\| + \varepsilon_1 + \varepsilon_2, \quad \varepsilon_2 > 0. \quad (34)$$

Remark 6: A salient feature of weight updating law (26) is the time-varying dead zone $\bar{\alpha}\|E(t)\|$. The updating algorithm stops when the operating point is inside the exponential tracking region according to the *Theorem 1* (i.e., $|\sigma(t)| < \bar{\alpha}\|E(t)\| < \alpha\|E(t)\|$); otherwise, the updating algorithm executes. The first term in the right-hand side of (26) is to deal with the uncertainties caused by the estimated weight error $\tilde{W}(t) = \bar{W} - W(t)$. Furthermore, its second term (or revised e-modification of [28]) is used to ensure the boundedness of estimated weight $W(t)$ without the requirement of PE (allude to the proof of this theorem) [16], [21], [28]. Hence, the conditions $\|\tilde{W}(0)\| < \rho_1$ and $\|x(0)\| < \rho_2$ are not necessary for small values of ρ_1 and ρ_2. From the result of the proof in the Appendix, the invariant set for the connection weight is described as follows: $\|\tilde{W}(t)\| < W_{\max}/2 + \sqrt{W_{\max}^2/4 + [\varepsilon_0\|\Phi(x,z)\| + \varepsilon_1]/\eta} < W_{\text{in}}$. If $\eta \to 0$, then $W_{\text{in}} \to \infty$. Hence, the η acts an important role for the convergent region of connection weight $W(t)$.

Remark 7: Substituting (33) and (34) into (29) and (30) gives

$$f_1(t) = \frac{\varepsilon_2(\alpha - \bar{\alpha})\|E(t)\|}{2\left[\eta W_{\max}^2/4 + (\varepsilon_0\|\Phi(x,z)\| + \varepsilon_1)\right]} + \frac{\varepsilon_2}{2\gamma_1}$$
$$f_2(t) = \frac{\varepsilon_2(\alpha - \bar{\alpha})\|E(t)\|}{\gamma_1}.$$

In general, $f_2(t) \ll f_1(t)$ if ε_2 and $1/\gamma_1$ is sufficiently small. Then, $f(t) \approx 0.5 f_2(t)/f_1(t)$. Hence,

$$f(t) = \frac{\mu(t)\left[\eta W_{\max}^2/4 + \varepsilon_0\|\Phi(x,z)\| + \varepsilon_1\right]}{\mu(t)\gamma_1 + \varepsilon_2} < \frac{\eta W_{\max}^2/4 + \varepsilon_0\|\Phi(x,z)\| + \varepsilon_1}{\gamma_1}$$
$$f(t) = \frac{\varepsilon_2(\alpha - \bar{\alpha})\|E(t)\|}{\mu(t)\gamma_1 + \varepsilon_2} < (\alpha - \bar{\alpha})\|E(t)\|.$$

If $\mu(t)\gamma_1 < \varepsilon_2$, then $f(t) < \alpha\|E(t)\| - \bar{\alpha}\|E(t)\| < \{\eta W_{\max}^2/4 + \varepsilon_0\|\Phi(x,z)\| + \varepsilon\}/\gamma_1$. That is, the condition 4) in *Theorem 3* can be satisfied after a suitable selection of control parameters. In addition, the condition 4) can be relaxed if $f(t) + \bar{\alpha}\|E(t)\| < \alpha\|E(t)\|$ is considered for the time-varying dead zone, i.e., $\Delta(t) = \alpha\|E(t)\| - f(t)$. However, the stability of the closed loop becomes complex.

Remark 8: As compared with the equivalent control $u_{\text{eq}}(t)$ in (12), (24) has an extra term $W^T(t)\Phi(x,z)$ to deal with the uncertainties. Moreover, the switching control $u_{\text{sw}}(t)$ in (25) is a smooth (or continuous) function; no chattering control input occurs [7], [9].

IV. Simulations and Discussions

The electrohydraulic servosystem with the following nominal parameters:

$$P_s = 13.795 \text{ Mpa}, \quad \beta_e = 344.875 \text{ Mpa}$$
$$V_t = 1.639 \times 10^{-4} \text{ m}^3$$
$$K_{\text{ce}} = 2.376 \times 10^{-6} \text{ Mpa}^{-1} \cdot \text{s}^{-1} \cdot \text{m}^3$$
$$D_m = 8.195 \times 10^{-6}, \quad J_t = 5.652 \times 10^{-2} \text{ N} \cdot \text{m} \cdot \text{s}^2$$
$$B_m = 8.477 \text{ m} \cdot \text{N} \cdot \text{s}, \quad K_v = 0.508 \text{ mV}^{-1}$$
$$G = 1.13 \times 10^{-3} \text{ m} \cdot \text{N} \cdot \text{rad}^{-1}, \quad \rho = 850 \text{ kg} \cdot \text{m}^{-3}$$
$$C_d = 0.67, \quad A_g = 3.385 \times 10^{-7} \text{ m}$$

and subject to an external load $T_l = 2\sin(4\theta_m)$ N·m, is simulated by the fourth-order Runge–Kutta method with 0.01-s time interval. The desired trajectory is assigned $\theta_d(t) = 5^\circ \sin(2\pi t)$ [5]. The coefficients of system (9) are described as follows: $\bar{a}_1(t) = 0.399\,82$ s^{-3}, $\bar{a}_2(t) = 13\,000.2711$ s^{-2}, $\bar{a}_3(t) = 169.980\,43$ s^{-1}. The system contains poles 0, $-84.9902 \pm j76.0061$ which are not all in a well-damped region. The control gain $b(t)$ and external load $d(t)$ are dependent on the state. Assume that the above servosystem is subject to the following parameter variations: $|\Delta a_i(t)| \le |\bar{a}_i(t)| = \alpha_i$, for $i = 1, 2, 3$. Furthermore, the upper bound of uncertain control gain and related external load are expressed as follows: $|\Delta b(t)| \le 0.5|\bar{b}(t)| = \beta(t)$ s^{-3}·V^{-1} and $\gamma(t) = |d(t)|$ s^{-3}. The initial value of state and connection weight is $x(0) = [0\ 0\ 0]^T$ and $W(0) = 0$. The stable switching surface with the following coefficients: $p_1 = 90$, $p_2 = 2600$, and $p_3 = 24\,000$ (i.e., the poles at -20, -30, and -40) is chosen. The compact subset is $\Omega(x,z) = \{x(t) : |x_1(t)| \le 2, |x_2(t)| \le 4, |x_3(t)| \le 16, \|z(t)\| \le 30\}$. The center of the jth kernel of the neural network for the normalized state (i.e., $x_1(t)/(6.25\,dr)$, $x_2(t)/(12.5\pi\,dr)$, and $x_3(t)/(25\pi^2\,dr)$, where $dr = \pi/180$ denotes the conversion factor between degree and radian) is $c_j = [c_{j1}\ \ c_{j2}\ \ c_{j3}]$, $1 \le j \le n = 125$, and its elements c_{ji} $(1 \le i \le 3) \in [-1\ \ -0.5\ \ 0\ \ 0.5\ \ 1]$. The width of nodes for the neural network is $\delta_i = 0.5, 1 \le i \le 125$. The upper bound of unknown connection weight is assumed to be $W_{\max} = 4$ and the value of α is assigned as 250.

Let $\Delta a_i(t) = \alpha_i$, $i = 1, 2, 3$, and $\Delta b(t) = 0.5\beta(t)$; i.e., 100% and 50% of bias for the parameter variations which are not the signals with PE. The following control parameters: $\eta = 0.25$, $h_{ii} = 1$, $\gamma_1 = 100$, $\bar{\alpha} = 5$, $\varepsilon_0 = 0.1$, $\varepsilon_1 = 0.1$, and $\varepsilon_2 = 0.01$ are used to achieve the simulated responses shown in Fig. 2. The proposed control scheme not only has the superior steady-state tracking accuracy, but also possesses acceptable transient performance. The maximum tracking error after transient response is about 0.08°, which is 1.6% of the amplitude of the desired trajectory (see the solid line in Fig. 4). The control input is smooth. The operating point is in the neighborhood of the switching surface due to the time-varying feature of the desired trajectory. The uncertainties in Fig. 2(d) are indeed huge; the learning uncertainties using the proposed neural network capture the dominant feature of the uncertainties. Owing to the advantage of the VSC, the excellent tracking performance in Fig. 2(a) is accomplished under the subjection of tremendous uncertainties. The connection weights are all bounded and they will be shown later. Moreover, no prior training requirement for the connection weight makes the control problems more practical to implement.

Because the traditional VSC cannot deal with the system with huge uncertainties, the time histories for the Fig. 2 case using the control law in *Theorem 1* are unbounded. The time

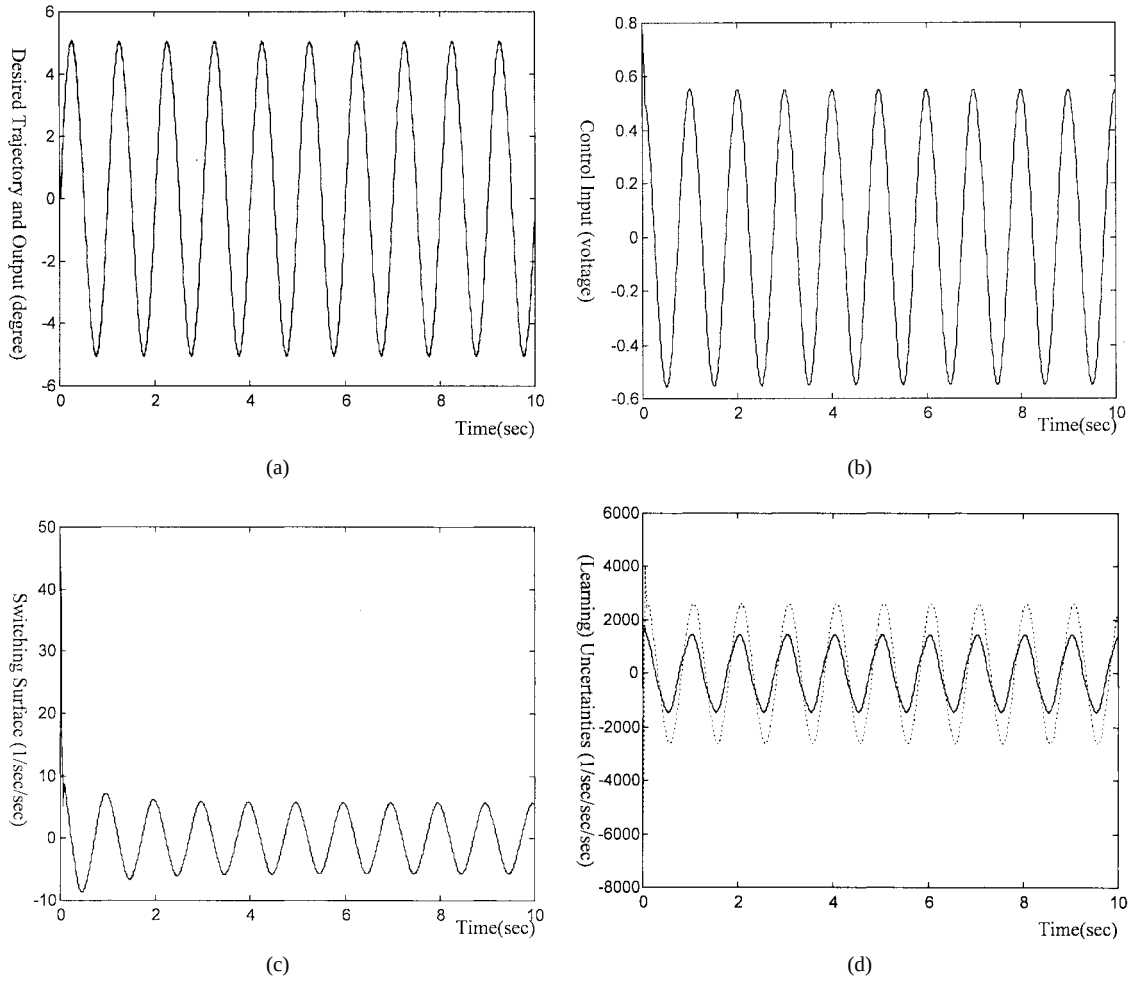

Fig. 2. Time histories of neural-network-based variable structure control with $p_1 = 90, p_2 = 2600, p_3 = 24000, \eta = 0.25, h_{ii} = 1, \bar{\alpha} = 5, \gamma_1 = 100$ for the system subject to parameter variations of 100% bias except 50% bias of parameter b and external load $T_l = 2\sin(4\theta_m)$. (a) $\theta_d(t)(\cdots)$ and $\theta_m(t)$(—). (b) $u(t)$. (c) $\sigma(t)$. (d) $\sum_{i=1}^{3} \Delta a_i(t)x_i(t) - \Delta b(t)u_{\mathrm{eq}}(t) + d(t) - \xi(t)$ (- - -) and $W^T(t)\Phi(x,z)$(___).

histories for the system subject to small parameter variations (e.g., 40% bias) and the external load $T_l = 2\sin(4\theta_m)$ N·m using the control in *Theorem 1* are shown in Fig. 3. Furthermore, the time histories of the Fig. 3 case with uncertainties larger than 45% bias will be unbounded. Comparing the results of Figs. 2 and 3, the following conclusions are given: 1) the tracking performance of the traditional VSC is often poor, as the system is subject to tremendous uncertainties (see Figs. 2 and 3); 2) the control input of the traditional VSC in the presence of huge uncertainties is always chattering and given too much to the system, resulting in the oscillatory response of system output [see Figs. 3(a) and (b)]; and 3) from the fact of 2), the operating point is not in the vicinity of switching surface as compared with Fig. 2(c).

In the sequence, the effects of the control parameters in *Theorem 3*, γ_1, η, $\bar{\alpha}$, ε_0, and ε_1 are investigated. If control parameter $\gamma_1 = 100$ in the Fig. 2 case is changed to $\gamma_1 = 200$, its maximum tracking error (i.e., 0.05° after a short transient period) is smaller than that in the Fig. 2 case (i.e., 0.08° after a short transient duration, see Fig. 4). However, its transient response of control input is larger than that in the Fig. 2 case (comparison between Figs. 2(b) and 5). If control parameter $\eta = 0.25$ in the Fig. 2 case is changed to $\eta = 0$, its maximum tracking error (i.e., 0.05° after a short transient interval) is smaller than that in the Fig. 2 case (i.e., 0.08° after a short transient period, see Fig. 4). However, the time histories of steady state for $\eta = 0$ contain higher frequencies as compared with that for $\eta = 0.25$. In addition, the time histories of connection weight for $\eta = 0$ are possibly unbounded (refer to the dashed line in Fig. 6). It could be dangerous if the controller keeps executing. Furthermore, if the dead zone for the update of connection weight is set to zero simultaneously (i.e., $\eta = \bar{\alpha} = 0$), the responses of connection weight diverge faster than those without e-modification in (26) (i.e., $\eta = 0, \bar{\alpha} = 5$ allude to Fig. 6). The larger value of η which occurs, the more oscillatory response and the faster convergence to zero of connection weight happens (see solid lines and dashed-double-dot lines in Fig. 6). The effect of the size of the dead zone (i.e., $\bar{\alpha}$) are presented in Fig. 7. From Fig. 7, the more oscillatory response of connection weight for the smaller value of $\bar{\alpha}$ is obtained; in addition, the response of connection weight for smaller value of $\bar{\alpha}$ can more approach the optimal (or true) value of connection weight. If control parameters $\varepsilon_0 = 0.1$ and $\varepsilon_1 = 0.1$ in the Fig. 2 case are changed to $\varepsilon_0 = 1$ and $\varepsilon_1 = 0.5$ or $\varepsilon_0 = 5$ and $\varepsilon_1 = 2$, their responses are similar to those in Fig. 2. For brevity, those

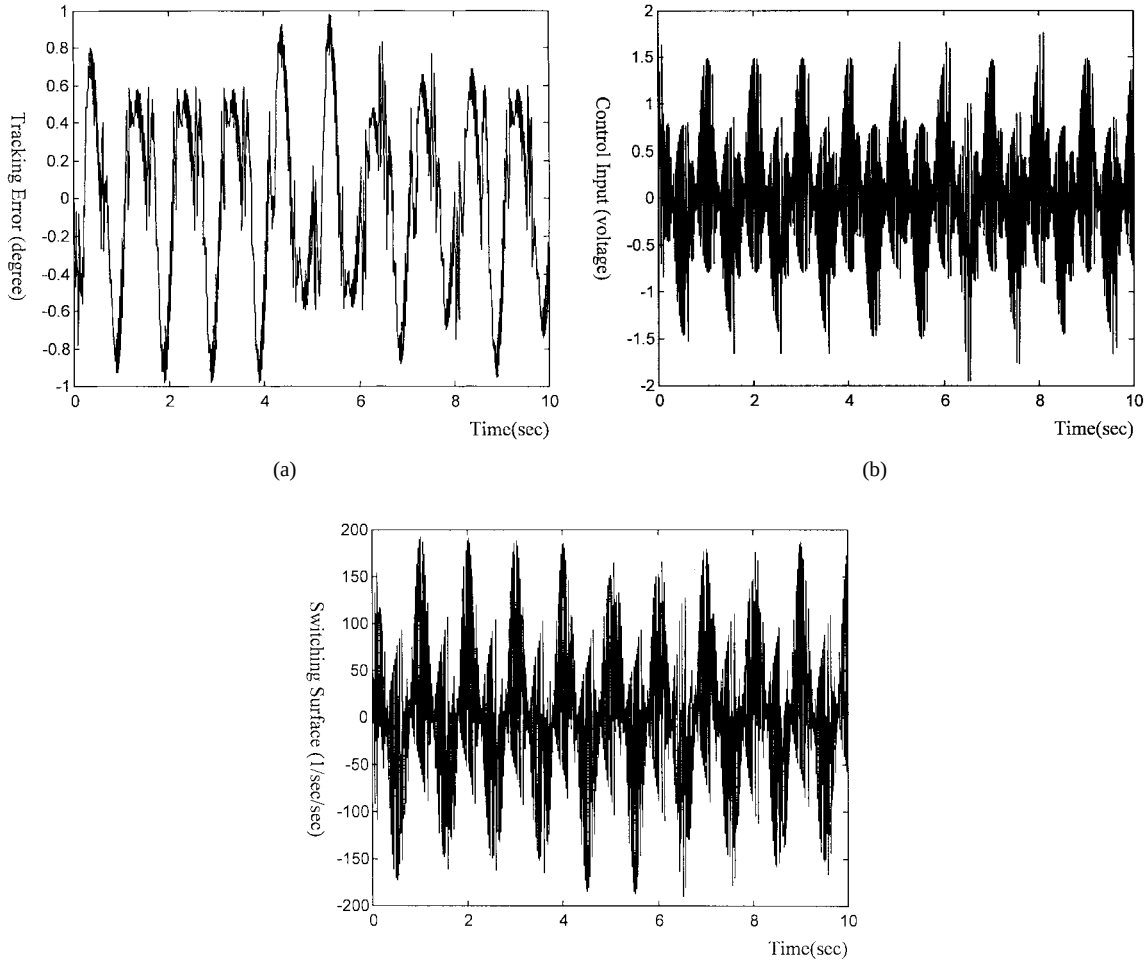

Fig. 3. Time histories of traditional VSC for the system subject to parameter variations 40% bias and external load $T_l = 2\sin(4\theta_m)$. (a) $\theta_d(t) - \theta_m(t)$. (b) $u(t)$. (c) $\sigma(t)$.

are left out. In short, a small value of η should be chosen to prevent the possible divergence of connection weight. Too large a value of η deteriorates the tracking performance owing to the poor learning of uncertainties. The selection of $\bar{\alpha}$ is not very critical. To avoid the large transient response, the switching control gain γ_1 is chosen from a small one and then increases to enhance the tracking performance under the consideration of transient response. The selection of control parameters ε_0 and ε_1 is not strict.

If the parameter variations are changed into half of random signal and half of bias, the response of tracking performance [i.e., Fig. 8(a)] is still acceptable and its maximum tracking error is about 0.16°, which is twice that of the Fig. 2 case. The control input [i.e., Fig. 8(b)] is also smooth enough as compared with Fig. 2(b). The response of connection weight is bounded and has a similar response of the Fig. 2 case shown in Figs. 6 and 7. For simplicity, those are omitted.

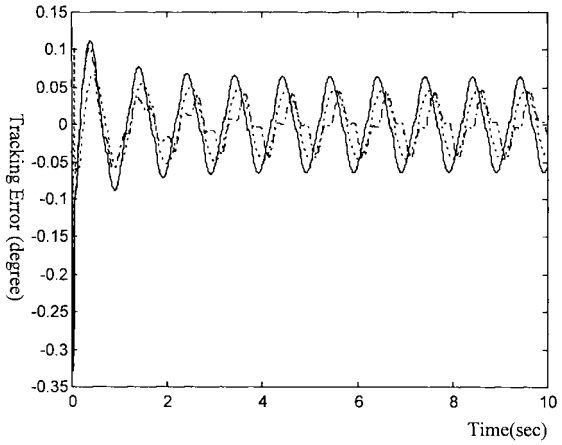

Fig. 4. Time histories of tracking error for NNBVSC of Fig. 2 case with different control parameters: ___ for $\gamma_1 = 100$, $\eta = 0.25$, --- for $\gamma_1 = 200$, $\eta = 0.25$, and -.-.- for $\gamma_1 = 100$, $\eta = 0$.

V. Conclusion

The reason for a chattering control input is that the switching control in the VSC is used to deal with the uncertainties of electrohydraulic servosystems caused by parameter variations, friction, external load, and controller. The larger the uncertainties which arise, the larger the switching control which occurs. In this paper, an RBFNN has been applied to model these uncertainties. A new adaptation law using a revision of e-modification by a time-varying dead zone can achieve an exponential stability without the assumption of PE for the

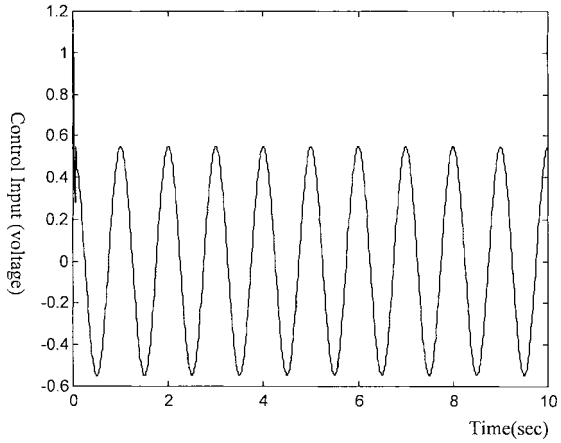

Fig. 5. Time histories of control input for NNBVSC of Fig. 2 case, except control parameter $\gamma_1 = 200$.

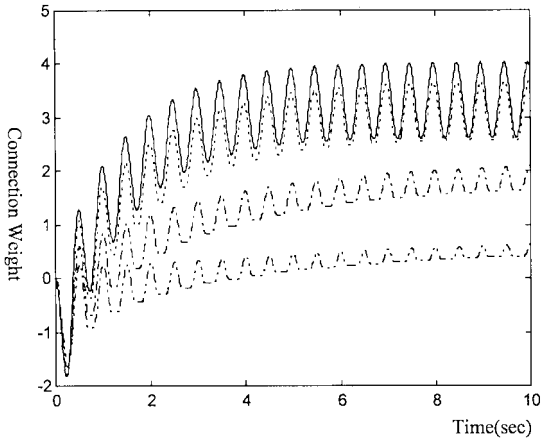

Fig. 7. Time histories of typical weight $w_{128}(t)$ for NNBVSC of the Fig. 2 case with different control parameter $\bar{\alpha}$: ___ for $\bar{\alpha} = 5$, --- for $\bar{\alpha} = 50$, -.-.- for $\bar{\alpha} = 150$, and -..-.. for $\bar{\alpha} = 220$.

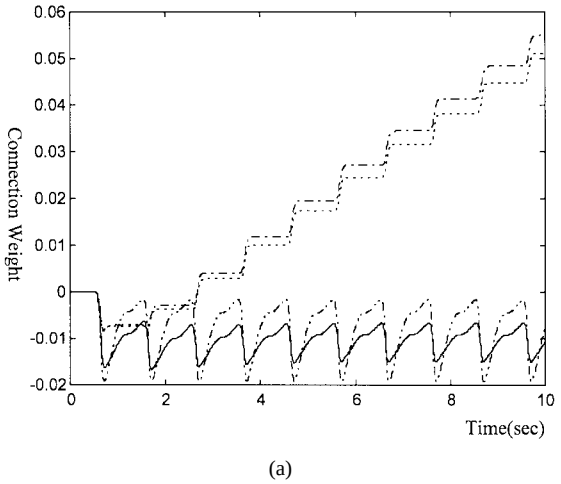

(a)

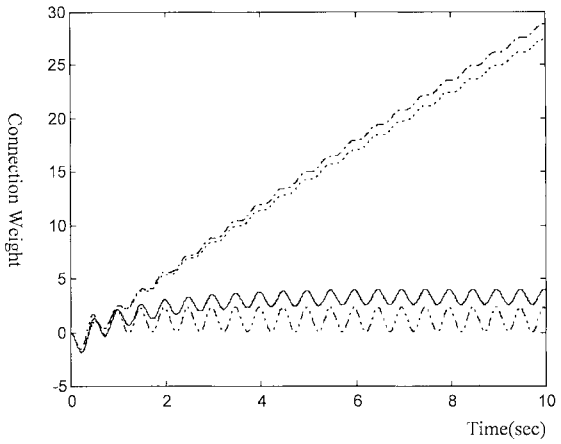

(b)

Fig. 6. Time histories of typical weights $w_1(t)$ and $w_{128}(t)$for NNBVSC of Fig. 2 case with different control parameters: ___ for $\eta = 0.25$, $\bar{\alpha} = 5$,--- for $\eta = 0$, $\bar{\alpha} = 5$, -.-.- for $\eta = 0$, $\bar{\alpha} = 0$, and -..-.. for $\eta = 0.5$, $\bar{\alpha} = 5$. (a) $w_1(t)$. (b) $w_{128}(t)$.

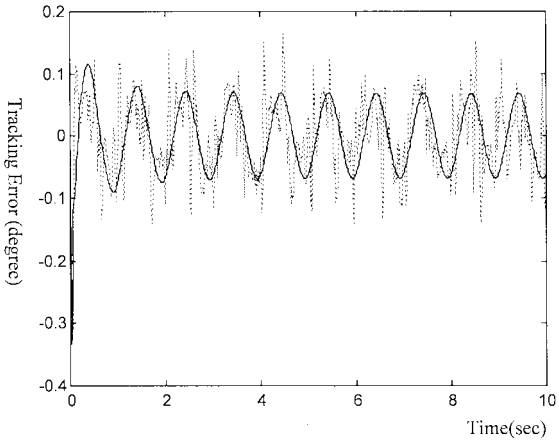

(a)

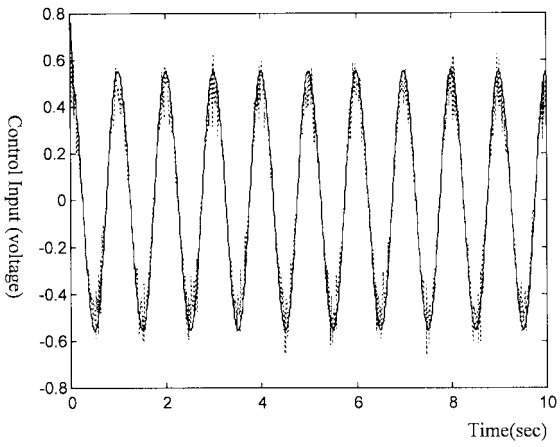

(b)

Fig. 8. Time histories for NNBVSC of the Fig. 2 case (——) with different parameter variations: half bias and half random (---). (a) $\theta_d(t) - \theta_m(t)$. (b) $u(t)$.

uncertainties or radial basis function. Then, an RBFNN-based VSC was designed. As compared with the traditional VSC, the proposed NNBVSC can cope with extra uncertainties to obtain an excellent tracking result without the occurrence of chattering control input. Furthermore, without the prior estimation of connection weight (e.g., off-line training) the initial weight is set to zero (i.e., no compensation for extra uncertainties with respect to VSC). This feature makes the proposed control scheme more practical to implement. The simulations also confirm the usefulness of the proposed controller. The author

believes that the proposed control can be applied to many practical control problems to ameliorate their performance (e.g., control of biped locomotion robot [30]).

APPENDIX

Proof of Theorem 3

If there are no ambiguities, the arguments of variables are omitted. Define the following Lyapunov function:

$$V(\sigma_\Delta, \tilde{W}) = \left(\sigma_\Delta^2 + \tilde{W}^T H \tilde{W}\right)/2 > 0, \quad \text{as } \sigma_\Delta \neq 0 \quad \text{or} \quad \tilde{W} = \bar{W} - W \neq 0. \tag{A1}$$

Taking the time derivative of (A1) and using (26) and (27) gives

$$\dot{V} = \sigma_\Delta \dot{\sigma}_\Delta + \tilde{W}^T H \dot{\tilde{W}} = \sigma_\Delta \dot{\sigma}_\Delta - \tilde{W}^T(\sigma_\Delta \Phi - \eta |\sigma_\Delta| W). \tag{A2}$$

If $|\sigma| \leq \Delta = \bar{\alpha}\|E\| < \alpha\|E\|$, then $\dot{V} = 0$. Obviously, the exponential stability of *Theorem 2* is obtained, i.e., $e(t) \to 0$ with a rate $(K_2 - \alpha K_1)$ as $t \geq t_0$. Similarly, the case $|\sigma| > \Delta = \bar{\alpha}\|E\|$ is derived as follows. From (27),

$$\dot{\sigma}_\Delta = \dot{\sigma} - \xi. \tag{A3}$$

Substituting (A3) into (A2) and using (8), (10), (21)–(26) and Assumptions A1–A5, gives

$$\begin{aligned}
\dot{V} &= \sigma_\Delta\{\ddot{\theta}_d + a_1 x_1 + a_2 x_2 + a_3 x_3 - [\bar{b} + \Delta b]u \\
&\quad + d + p_1 \ddot{e} + p_2 \dot{e} + p_3 e - \xi\} - \tilde{W}^T(\sigma_\Delta \Phi - \eta|\sigma_\Delta| W) \\
&= \sigma_\Delta \left\{ \sum_{i=1}^{3} \Delta a_i x_i + d - \Delta b u_{\text{eq}} - \xi - W^T \Phi - [\bar{b} + \Delta b] u_{\text{sw}} \right\} \\
&\quad - \tilde{W}^T(\sigma_\Delta \Phi - \eta|\sigma_\Delta| W) \\
&= \sigma_\Delta \left\{ \tilde{W}^T \Phi + \varepsilon - \frac{[\bar{b} + \Delta b]}{[\bar{b} - \beta]} \left[\gamma_1 \sigma_\Delta + \frac{\gamma_2 \sigma_\Delta}{|\sigma_\Delta| + \mu} \right] \right\} \\
&\quad - \tilde{W}^T(\sigma_\Delta \Phi - \eta|\sigma_\Delta| W) \\
&\leq |\sigma_\Delta| \left\{ \varepsilon_0 \|\Phi\| + \varepsilon_1 - \left[\gamma_1 |\sigma_\Delta| + \frac{\gamma_2 |\sigma_\Delta|}{|\sigma_\Delta| + \mu} \right] + \eta \tilde{W}^T [\bar{W} - \tilde{W}] \right\} \\
&\leq \frac{-\gamma_1 |\sigma_\Delta|}{|\sigma_\Delta| + \mu} \left\{ \frac{\gamma_2 |\sigma_\Delta|}{\gamma_1} + |\sigma_\Delta|(|\sigma_\Delta| + \mu) \right. \\
&\quad \left. - \frac{(|\sigma_\Delta| + \mu)[(\varepsilon_0 \|\Phi\| + \varepsilon_1) + \eta \|\tilde{W}\|(W_{\max} - \|\tilde{W}\|)]}{\gamma_1} \right\} \\
&\leq \frac{-\gamma_1 |\sigma_\Delta|}{|\sigma_\Delta| + \mu} \left\{ \frac{\eta(|\sigma_\Delta| + \mu)[\|\tilde{W}\| - W_{\max}/2]^2}{\gamma_1} \right. \\
&\quad - \frac{(|\sigma_\Delta| + \mu)\left[\eta W_{\max}^2 + (\varepsilon_0 \|\Phi\| + \varepsilon_1)\right]}{\gamma_1} \\
&\quad \left. + |\sigma_\Delta|(|\sigma_\Delta| + \mu) + \frac{\gamma_2 |\sigma_\Delta|}{\gamma_1} \right\} \\
&\leq \frac{-\gamma_1 |\sigma_\Delta|}{|\sigma_\Delta| + \mu} \left\{ \frac{\eta(|\sigma_\Delta| + \mu)[\|\tilde{W}\| - W_{\max}/2]^2}{\gamma_1} + F(|\sigma_\Delta|) \right\}
\end{aligned} \tag{A4}$$

where

$$F(|\sigma_\Delta|) = |\sigma_\Delta|^2 + 2 f_1 |\sigma_\Delta| - f_2. \tag{A5}$$

Then, from (A4), either $F(|\sigma_\Delta|) > 0$, or $\|\tilde{W}\| > W_{\max}/2 + \sqrt{W_{\max}^2/4 + (\varepsilon_0\|\Phi\| + \varepsilon_1)/\eta}$ makes $V < 0$.

If $F(|\sigma_\Delta|) > 0$, the operating point eventually converges into the neighborhood of the switching surface, i.e., $|\sigma_\Delta|(t) < f(t)$ for $t \geq t_0$. To ensure the exponential tracking based on *Theorem 2*, $|\alpha| < \alpha\|E\|$ should be satisfied. Then, from (27), the condition 4), and triangle inequality, $|\sigma| \leq |\sigma_\Delta| + \bar{\alpha}\|E\| < f + \bar{\alpha}\|E\| < \alpha\|E\| < \{\eta W_{\max}^2/4 + \varepsilon_1\|\Phi\| + \varepsilon_0\}/\gamma_1 + \bar{\alpha}\|E\|$ is obtained. The solution of μ from the inequality $f + \bar{\alpha}\|E\| < \alpha\|E\|$ gives the result of (32). Furthermore, the satisfaction of condition 4) $\{\eta W_{\max}^2/4 + \varepsilon_0\|\Phi\| + \varepsilon_1\}/\gamma_1 + \bar{\alpha}\|E\| > \alpha\|E\|$ ensures a positive boundary layer μ in (32).

If $\|\tilde{W}\| > W_{\max}/2 + \sqrt{W_{\max}^2/4 + (\varepsilon_0\|\Phi\| + \varepsilon_1)/\eta}$, the estimation error of connection weight ultimately converges to the vicinity of zero (i.e., $\|\tilde{W}\| < W_{\max}/2 + \sqrt{W_{\max}^2/4 + (\varepsilon_0\|\Phi\| + \varepsilon_1)/\eta}$). Hence, the estimation of connection weight $\{W(t)\}$ is bounded because of the fact (21).

Therefore, either $|\sigma_\Delta(t)|$ or $\|\tilde{W}\|$ increases too much, and the Lyapunov function decreases so that both $|\sigma_\Delta(t)|$ and $\|\tilde{W}\|$ decrease as well. From (23) to (32), $\{u(t)\}$ is bounded. □

ACKNOWLEDGMENT

The author would like to thank the reviewers for their comments and suggestions.

REFERENCES

[1] H. E. Merritt, *Hydraulic Control System*. New York: Wiley, 1976.
[2] J. Watton, "The general responses of servovalve-controlled single-rod, linear actuator and influence of transmission line dynamics," *ASME J. Dynam. Syst., Measur., Contr.*, vol. 106, pp. 157–162, 1984.
[3] H. M. Handoos and M. J. Vilenius, "The utilization of experimental data in modeling hydraulic single stage pressure control valves," *ASME J. Dynam. Syst., Measur., Contr.*, vol. 112, pp. 482–488, 1990.
[4] S. T. Tsai, A. Akers, and S. J. Lin, "Modeling and dynamic evaluation of a two-stage two-spool servovalve used for pressure control," *ASME J. Dynam. Syst., Measur., Contr.*, vol. 113, pp. 709–713, 1991.
[5] T. Higuchi, T. Yamaguchi, I. Maehara, and K. Saito, "Development of a high speed noncircular machining NC-lathe by electrohydraulic servomechanism," *JSPE*, vol. 56, no. 2, pp. 293–297, 1990.
[6] S. W. Lee and J. H. Kim, "Robust adaptive stick-slip friction compensation," *IEEE Trans. Ind. Electron.*, vol. 42, no. 5, pp. 474–479, 1995.
[7] C. L. Hwang, "Fourier series neural-network-based adaptive variable structure control for servosystems with friction," *Proc. Inst. Elect. Eng.*, vol. 144, pt. D, no. 6, pp. 559–565, 1997.
[8] T. L. Chern and Y. C. Wu, "Design of integral variable structure controller and application to electrohydraulic velocity servosystems," *Proc. Inst. Elect. Eng.*, vol. 138, pt. D, no. 5, pp. 439–443. 1991.
[9] C. L. Hwang, "Sliding mode control using time-varying switching gain and boundary layer for electrohydraulic position and differential pressure control," *Proc. Inst. Elect. Eng.*, vol. 143, pt. D, no. 4, pp. 325–332, 1996.
[10] S. R. Lee and K. Srinivasan, "Self-tuning control application to closed-loop servohydraulic material testing," *ASME J. Dynam. Syst., Measur., Contr.*, vol. 112, pp. 680–689, 1990.
[11] J. S. Yun and H. S. Cho, "Application of an adaptive model following control technique to a hydraulic servo system subjected to unknown disturbances," *ASME J. Dynam. Syst., Measur., Contr.*, vol. 113, pp. 479–486, 1991.
[12] F. Harashima, H. Hashimoto, and S. Kondo, "MOSFET converter-fed position servo system with sliding mode control," *IEEE Trans. Ind. Electron.*, vol. 32, no. 3, pp. 238–244, 1985.

[13] J. J. E. Slotine and J. A. Coetsee, "Adaptive sliding controller synthesis for nonlinear systems," *Int. J. Contr.*, vol. 43, no. 6, pp. 1631–1651, 1986.
[14] P. Kachroo and M. Tomizuka, "Chattering reduction and error convergence in the sliding-mode control of a class of nonlinear systems," *IEEE Trans. Automat. Contr.*, vol. 32, no. 7, pp. 1063–1068, 1996.
[15] S. Oucheriah, "Robust sliding mode control of uncertain dynamic delay systems in the presence of matched and unmatched uncertainties," *ASME J. Dynam. Syst., Measur., Contr.*, vol. 119, pp. 69–72, 1997.
[16] S. Jagannathan and F. L. Lewis, "Multilayer discrete-time neural-net controller with guaranteed performance," *IEEE Trans. Neural Networks*, vol. 7, pp. 107–130, Jan. 1997.
[17] R. M. Sanner and J. J. E. Slotine, "Gaussian network for direct adaptive control," *IEEE Trans. Neural Networks*, vol. 3, pp. 837–863, Nov. 1992.
[18] S. Fabri and V. Kadirkkamanathan, "Dynamic structure neural networks for stable adaptive control of nonlinear systems," *IEEE Trans. Neural Networks*, vol. 12, pp. 1151–1167, Sept. 1996.
[19] C. L. Hwang and F. Y. Sung, "Neuro-observer controller design for nonlinear dynamical systems," in *Proc. 35th IEEE Conf. Decision and Control*, Kobe, Japan, Dec. 10–12, 1996, pp. 3310–3316.
[20] N. Sadegh, "A perceptron network for functional identification and control of nonlinear systems," *IEEE Trans. Neural Networks*, vol. 12, pp. 837–863, Sept. 1992.
[21] F. L. Lewis, K. Liu, and A. Yesildirek, "Neural net robot controller with guaranteed tracking performance," *IEEE Trans. Neural Networks*, vol. 6, pp. 703–715, May 1995.
[22] E. B., M. M. Polycarpou, M. A. Christodoulou, and P. A. Ioannou, "High-order neural network structures for identification of nonlinear dynamical systems," *IEEE Trans. Neural Networks*, vol. 6, pp. 422–431, Mar. 1995.
[23] F. C. Chen and H. K. Khalil, "Adaptive control of a class of nonlinear discrete-time systems using neural network," *IEEE Trans. Automat. Contr..*, vol. 40, pp. 791–801, May 1995.
[24] B. Egardt, *Stability of Adaptive Controllers*. New York: Springer-Verlag, 1979.
[25] B. B. Peterson and K. S. Narendra, "Bounded error adaptive control," *IEEE Trans. Automat. Contr.*, vol. 27, pp. 1161–1168, Dec. 1982.
[26] G. Kreisselmeier and B. D. O. Anderson, "Robust model reference adaptive control," *IEEE Trans. Automat. Contr.*, vol. 31, pp. 127–133, Feb. 1986.
[27] P. A. Ioannou and P. V. Kokotovic, *Adaptive Systems with Reduced Models*. New York: Springer-Verlag, 1983.
[28] K. S. Narendra and A. M. Annaswamy, "A new adaptation law for robust adaptation without persistent excitation," *IEEE Trans. Automat. Contr.*, vol. 32, pp. 134–145, Feb. 1987.
[29] D. Gorinevsky, "On the persistency of excitation in radial basis function network identification of nonlinear systems," *IEEE Trans. Neural Networks*, vol. 6, pp. 1237–1244, Sept. 1995.
[30] J. Furusho and M. Masubuchi, "A theoretically motivated reduced order model for the control of dynamic biped locomotion," *ASME J. Dynam., Syst., Measur., Contr.*, vol. 109, pp. 155–163, 1987.

Chih-Lyang Hwang (M'95–A'96) received the B.E. degree in aeronautical engineering from Tamkang University, Taipei, Taiwan, R.O.C., in 1981, and the M.E. and Ph.D. degrees in mechanical engineering from Tatung Institute of Technology, Taipei, Taiwan, R.O.C., in 1986 and 1990, respectively.

Since 1990, he has been with the Department of Mechanical Engineering, Tatung Institute of Technology, where he is engaged in teaching and research in the area of servocontrol and control of manufacturing systems and has been a Professor since 1996. From August 1998 to February 1999, he was a Research Scholar, in the Department of Mechanical Engineering, Georgia Institute of Technology, Atlanta. Also, since 1996, he has been a Referee of Patents for the National Standards Bureau, Ministry of Economy of Taiwan. He is the author or coauthor of several journal papers. His current research interests include neural network modeling and control, variable structure control, fuzzy control, mechatronics, and robotics.